Engineering Negative Differential Conductance with the Cu(111) Surface State

B. W. Heinrich,[1,*] M. V. Rastei,[1] D.-J. Choi,[1] T. Frederiksen,[2] and L. Limot[1,†]

[1]*Institut de Physique et Chimie des Matériaux de Strasbourg, CNRS Université de Strasbourg, F-67034 Strasbourg, France*
[2]*Donostia International Physics Center (DIPC), E-20018 Donostia-San Sebastián, Spain*

Low-temperature scanning tunneling microscopy and spectroscopy are employed to investigate electron tunneling from a C_{60}-terminated tip into a Cu(111) surface. Tunneling between a C_{60} orbital and the Shockley surface states of copper is shown to produce negative differential conductance (NDC) contrary to conventional expectations. NDC can be tuned through barrier thickness or C_{60} orientation up to complete extinction. The orientation dependence of NDC is a result of a symmetry matching between the molecular tip and the surface states.

PACS numbers: 73.63.−b, 68.37.Ef, 72.80.Rj, 73.20.At

Important advances have been made over the past decades in molecular electronics. Among these is the demonstration that molecules can perform controllable functions such as negative differential resistance or conductance (NDC) [1–3]. First discovered in the Esaki diode [4], NDC leads to regions in the *I-V* curve where the current *I* decreases (increases) with increasing (decreasing) voltage *V*. This fundamental property is nowadays exploited in complementary metal-oxide-semiconductor devices for low-power memory, fast switches or oscillators. Early atomic-scale observations of NDC by scanning tunneling microscopy (STM) have been attributed to narrow energy states in tip and sample [5,6], in analogy with the resonant tunneling leading to NDC in semiconductors [7]. In principle, resonant tunneling via molecular orbitals also leads to NDC in single molecules [8–10], but progress in this direction has been hindered by the lack of microscopic control over electrode and molecule status.

It was shown, in particular, with single C_{60} that NDC occurrence can be improved by narrowing the molecular levels through a reduced molecule-substrate coupling [11,12], in order to exploit the bias dependence of the transmission function [13,14]. In this Letter, we introduce a different approach and report the occurrence of single-molecule NDC with a C_{60}-terminated tip. By attaching a molecule to the STM tip an increased control is gained over the entire tunnel junction [15,16]. This method allows, unlike previous NDC studies, exploring the NDC occurrence with well-defined pristine metal surfaces serving as a conterelectrode. Taking advantage of this setup, we demonstrate in stark contrast to conventional mechanisms that NDC can be produced by electron tunneling between a molecular orbital of the tip and a two-dimensional electron gas hosted by a copper surface—the Shockley surface states of Cu(111). In this calibrated setup, NDC may be tuned by varying the barrier thickness or by changing the C_{60} orientation up to complete extinction. Our study demonstrates that molecular orbitals act as angular momentum filters to the tunneling process, leading, in particular, to

NDC if accurately matched with the local orbital symmetry of the surface states. These findings should simplify NDC engineering at the atomic scale.

The measurements were carried out with an STM operating at 4.6 K in the 10^{-11} mbar range. After cleaning Cu(111) by sputter-anneal cycles, 0.15 monolayers of C_{60} were dosed onto the surface from a crucible containing a 99.9% pure powder heated to 400 °C. Single Au atoms were instead evaporated onto the cold surface by heating a high-purity gold wire. The differential conductance spectra, $dI/dV(V)$ were acquired via lock-in detection with a bias modulation ranging from 3 to 10 mV rms at 670 Hz (sample bias is measured with respect to the tip). The etched *W* tip employed was cleaned by sputter-anneal cycles and treated *in vacuo* by soft indentations into the clean surface. The tip apex was therefore coated with copper.

Figure 1(a) presents the electronic structure of the Cu(111) surface acquired with a metal tip (dashed line). Known spectroscopic features are evidenced [17]. The steplike feature at −0.45 V is associated to Shockley surface states, which are an experimental realization of a nearly two-dimensional electron gas; the marked upturn below −0.9 V is due to copper *d* states present below the (111) band gap. To engineer NDC with a C_{60} tip, we attach a single C_{60} to the copper-coated tip by repeatedly bringing the tip into contact with the target molecule and pressing beyond contact [15]. Figure 1(a) presents a conductance spectrum acquired with a C_{60} tip over Cu(111). The spectrum is nearly mirror symmetric to the spectrum acquired with a metallic tip positioned above a C_{60} molecule (compare with Fig. S2(b) in the Supplemental Material [18]). The lowest unoccupied molecular orbital is located at negative bias (LUMO: −0.5 V, LUMO + 1: −1.9 V), while the highest occupied molecular orbital is at positive bias (HOMO: 2.0 V, not shown). The widths of the molecular states are typically 0.5 V and compare well with a C_{60} molecule adsorbed on a metal surface [19–21]. Most importantly, NDC is detected below the LUMO + 1.
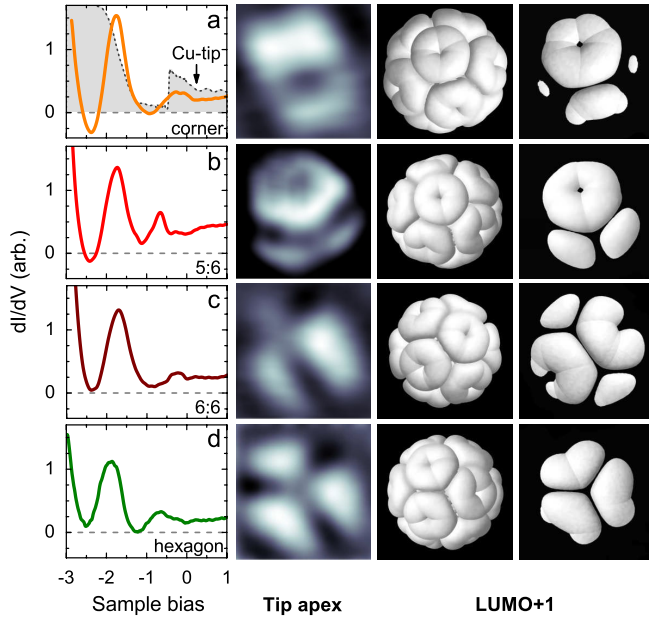
FIG. 1 (color online). (a)–(d) dI/dV over Cu(111) for various C_{60} tips (1.0 V, 0.1 nA). The orientation of C_{60} at each tip apex is determined by constant-current images over a Au atom (sample bias: -2.0 V, current: 0.1 nA, size: 12×12 Å^2). Each orientation is flanked by a Hückel simulation of the LUMO $+ 1$ orbital, and for better visibility, by the same orbital cut along the xy plane (the LUMO $+ 1$ orbital is localized on the pentagons forming the C_{60} skeleton). Panel (a) present also a dI/dV spectrum over Cu(111) acquired with a copper-coated W tip (dashed line, feedback loop opened at -3.0 V and 5 nA).

Among the numerous C_{60} tips investigated, the ones producing NDC had a specific C_{60} orientation relative to the copper surface. Figures 1(a)–1(d) summarize our findings. In order to image the tip apex, constant-current images of a Au atom were acquired [15]. These images exhibit a molecular pattern matching the LUMO $+ 1$ for biases close to -1.9 V. The orientations reported in Fig. 1 correspond to a C_{60} adsorbed on a carbon atom [labeled corner in Fig. 1(a)], on a pentagon-hexagon bond [5:6 in Fig. 1(b)], on a hexagon-hexagon bond [6:6 in Fig. 1(c)] and on a hexagonal ring [hexagon in Fig. 1(d)]. The apex C_{60} was rotated by performing a tip contact with a Au atom [22]. While the corner and the 5:6 adsorptions favor NDC, other orientations tend to suppress it. We also found that the interface structure between the C_{60} molecule and the copper tip has only a limited impact on NDC. Typical spectra acquired with different C_{60} tips, but with the same corner or 6:6 orientation are presented in Figs. 2(a) and 2(b), respectively. Despite the C_{60}-copper interface changes in these tips, as indicated by the shift of the LUMO and LUMO $+ 1$ (of the order of 0.5 and 0.2 V, respectively) [21], the dominant mechanism leading to NDC is still the C_{60} orientation.

Along with molecular orientation, counterelectrode selection is extremely crucial to NDC. In our setup, the
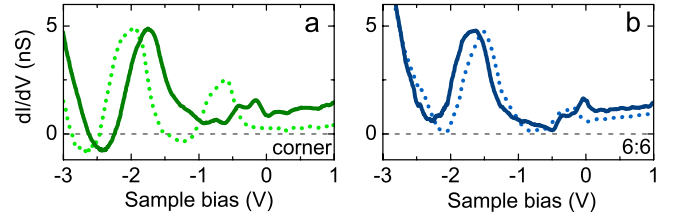

FIG. 2 (color online). dI/dV acquired above Cu(111) with two different tips (1.0 V, 1.0 nA), having (a) same corner orientation for C_{60} [as in Fig. 1(a)], (b) same 6:6 orientation for C_{60} [as in Fig. 1(c)].

counterelectrode can be conveniently chosen by positioning a C_{60} tip above nanoscale objects supported by Cu(111) or by changing the metal surface. We tested NDC occurrence with counterelectrodes having a featureless electronic structure over the energy range of interest, such as a Au atom on Cu(111) or the Cu(100) surface. We also tested counterelectrodes with a marked electronic structure like cobalt islands on Cu(111) [23], or a C_{60} molecule on Cu(111). None of the dI/dV spectra, presented as Supplemental Material [18], exhibited NDC. The fact that NDC is instead observed on Au(111) as on Cu(111) [24], indicates that electron tunneling into the Shockley surface states is likely a key mechanism behind NDC.

Motivated by recent studies [12,13,25], we also investigated the influence of barrier thickness on NDC. Figure 3(a) presents a typical set of spectra acquired at various distances, while Fig. 3(b) quantifies the changes in NDC with distance (noted z) for a collection of C_{60} tips. Through a tip displacement it is possible to tune NDC and, unlike previous work, even switch it off well within the tunneling regime at a distance of 3 Å from the surface. As
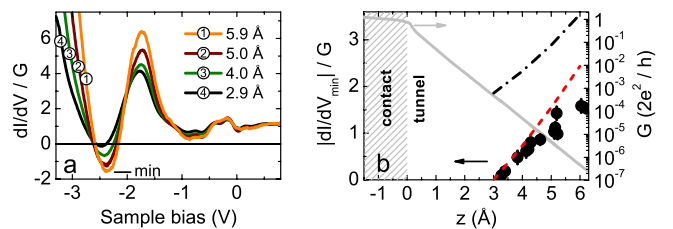

FIG. 3 (color online). (a) dI/dV spectra for various barrier thicknesses. The spectra are normalized by the conductance ($G = I/V$) at which the feedback loop was opened, respectively, from top to bottom: 0.01, 0.1, 1 and 10 nS. (b) NDC intensity versus tip-sample distance (left vertical axis) and corresponding changes of G (right vertical axis). From the tunneling regime, we extract an apparent-barrier height of $\Phi = 5$ eV. The distance is estimated by taking $z = 0$ for the contact conductance (G vs z curve acquired at 1 V), the hatched lines highlighting the contact regime. The NDC intensity corresponds to the minimum of the dI/dV curves in (a). The lines correspond to the simulation detailed in the text: a realistic DOS (dashed line) and a stepped DOS without d-bulk contribution (dash-dotted line).

established below, NDC extinction is a general property of our simplified setup not exclusive to C_{60}.

In the following we discuss the origin of the NDC with emphasis on the central role played by the Shockley surface states. To successfully engineer NDC, an accurate choice of the counterelectrode, of molecular orientation, and of barrier thickness turns out to be crucial. To start, we adopt a WKB framework and focus on a junction comprising a sample metal surface and a C_{60} tip with density of states (DOS) ρ_s and ρ_t, respectively. The zero-temperature current I as a function of sample voltage V is then

$$I(V, z) \propto \int_{E_F-V}^{E_F} \sum_m \rho_s^m(E + V)\rho_t^m(E)T(E, V, z)dE, \quad (1)$$

where $T(E, V, z) = \exp(-2\sqrt{2(\Phi - V/2 - E)}z)$ is the transmission function in Hartree atomic units. The explicit summation over magnetic quantum numbers m (projection of electron angular momentum on the common symmetry axis) excludes the extremely small probability for tunneling between states with different m [10,26]. For an accurate description of the tunneling current, we need just to distinguish between $m = 0$ and $m \neq 0$ in the DOS. This distinction is necessary as, near Γ, the sp-like Shockley surface states of Cu(111) only couple to the $m = 0$ component of the tip states. To model the sample DOS, we thus take a stepped function centered at -0.45 eV for the surface states and a low-energy exponential upturn for the copper bulk d states to represent $\rho_s^{m=0}$ [dashed line, negative half-plane, Fig. 4(a)] and a constant background plus exponential upturn for $\rho_s^{m\neq0}$ [dotted line, negative half-plane, Fig. 4(a)]. The total DOS (dash-dotted line) roughly mimics the electronic structure evidenced in Fig. 1(a). For the C_{60} tip we represent ρ_t as a set of three Lorentzian peaks for the HOMO, LUMO, and LUMO + 1 as described in the caption to Fig. 4(a). The $m = 0$ (dashed line) and $m \neq 0$ (dotted line) components sum up (thick line) to amplitudes proportional to the free-molecule degeneracies.

As shown in Fig. 4(b), the corresponding simulated dI/dV captures the essential experimental facts. There is indeed NDC in the spectrum just below the LUMO + 1 down to distances close to $z = 3$ Å. The role of the Shockley surface states in the NDC is evident from the energy-resolved current shown in Fig. 4(c): At a sample voltage $V = -2.35$ V the surface-state onset matches the LUMO + 1 resonance [5,6]. Upon a slight increase in the voltage the surface-state step feature moves away from the molecular resonance. The associated loss in energy-resolved current (dark orange [dark gray] area) is only partially compensated by the corresponding shift of the sample chemical potential (light orange [light gray] area), the tunnel current effectively *decreases* thus giving rise to NDC [27]. The comparison to our experimental results is also satisfying as shown by the dashed line in Fig. 3(b), where we also include the NDC produced by a stepped
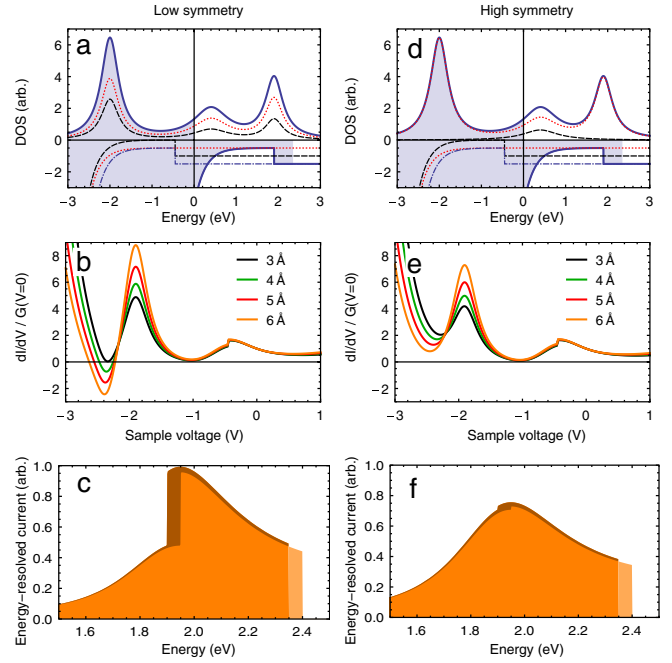

FIG. 4 (color online).   (a) DOS of a low-symmetry C_{60} tip (upper half-plane, thick line) and Cu(111) surface (lower half-plane, dash-dotted line: $V = 0$ V, thick line: $V = -2.35$ V) used in the WKB simulation ($m = 0$ and $m \neq 0$ components shown with dashed and dotted lines, respectively). Copper DOS: step function of unit amplitude centered at -0.45 eV in $\rho_s^{m=0}$ and a constant background set to 0.5 in $\rho_s^{m\neq0}$ with low-energy upturn. C_{60} DOS: three Lorentzian peaks mimicking the HOMO (-2.0 eV), LUMO (0.4 eV) and LUMO + 1 (1.9 eV) with widths 0.5 eV, 1.0 eV, and 0.5 eV, respectively, and amplitudes proportional to the free-molecule degeneracies (thick line). The occupied states are indicated by the shaded blue areas for the sample voltage $V = -2.35$ V where the Shockley surface-state edge matches the LUMO + 1 resonance. (b) Simulated dI/dV for (a) via Eq. (1). (c) Energy-resolved current for $V = -2.35$ V (dark orange [dark gray]) and $V = -2.40$ V (light orange [light gray]) for $z = 6$ Å. (d)–(f) Similar to (a)–(c) but for a high-symmetry C_{60} orientation where the $m = 0$ component is suppressed for HOMO and LUMO + 1.

function (dash-dotted line) without the d-bulk upturn. The increased NDC intensity without the d states highlights that they are detrimental to NDC. The peculiar decay reported in Fig. 3(b) is therefore the result of a competition between opposite effects for d states and Shockley surface states.

Another salient experimental finding is the impact of C_{60} orientation on NDC, which was set aside in the above discussion. In Fig. 1 it was found that NDC occurs with C_{60} in low-symmetry configurations (e.g., corner orientation) but disappears in high-symmetry configurations (e.g., hexagon orientation). Our NDC originates from the Shockley surface states which select $m = 0$ tip states. This suggests that for the high-symmetry C_{60} orientations the $m = 0$ component of the LUMO + 1 vanishes. Indeed

TABLE I. C_{60} orbitals in different local symmetries imposed by molecular orientation with respect to an isotropic surface.

	Isolated I_h	5:6/corner C_s	6:6 C_{2v}	Hexagon C_{3v}	Pentagon C_{5v}
HOMO	H_u	$2A' + 3A''$	$A_1 + 2A_2 + B_1 + B_2$	$A_2 + 2E$	$A_2 + E_1 + E_2$
LUMO	T_{1u}	$2A' + A''$	$A_1 + B_1 + B_2$	$A_1 + E$	$A_1 + E_1$
LUMO + 1	T_{1g}	$A' + 2A''$	$A_2 + B_1 + B_2$	$A_2 + E$	$A_2 + E_1$

such an effect can be rationalized by considering the transformation properties of the C_{60} tip orbitals using group theory as follows.

For isolated C_{60} molecules of icosahedral symmetry I_h the HOMO is a fivefold degenerate state of H_u symmetry while the LUMO and LUMO + 1 are triply degenerate states of T_{1u} and T_{1g} symmetry, respectively. When the molecule is adsorbed on a surface these degeneracies will be reduced [28], and, importantly here, the orbital angular momentum components onto the common symmetry axis perpendicular to the surface will depend on the molecular orientation. In Table I we list how the orbitals are split in different relevant local symmetry environments. For instance, a C_{60} molecule adsorbed with a hexagon on an isotropic surface possesses a threefold rotation axis and can thus be considered as belonging to the C_{3v} group. As a consequence it can be shown that the T_{1g} LUMO + 1 splits into $A_2 + E$ representations [29]. However, from the character table of C_{3v} it is evident that s, p_z, and d_{z^2} orbitals do not transform according to those representations. In other words, the LUMO + 1 does not have a $m = 0$ component for the hexagon orientation. Contrarily, a C_{60} molecule adsorbed on a 5:6 bond or a corner atom only possesses bilateral symmetry as described by C_s, and the LUMO + 1 is split into $A' + 2A''$. As s, p_z, and d_{z^2} do transform in C_s according to those representations the LUMO + 1 consequently contains a $m = 0$ component in these low-symmetry configurations.

More generally, based on Table I we can conclude that tunneling into the surface state is symmetry forbidden for orbitals which do not transform as the totally symmetric representation (A'/A_1), i.e., the HOMO for pentagon and hexagon orientations and the LUMO + 1 for 6:6, pentagon, and hexagon orientations. Note also that there are no such symmetry constraints for the LUMO orbital. To simulate the dI/dV recorded with C_{60} tips with high-symmetry orientation we therefore eliminated the $\rho_t^{m=0}$ component in the HOMO and LUMO + 1 [Fig. 4(d)]. As shown in Figs. 4(e) and 4(f), indeed this leads to the disappearance of NDC as was observed experimentally [Fig. 1(c) and 1(d)].

To summarize, we have shown that electron tunneling between a well-calibrated molecule and a two-dimensional electron gas produces a tunable NDC. By controlling both tip and sample states and accounting for their symmetries,

we demonstrated the concept of local orbital symmetry matching [10]. Barrier thickness or symmetry matching between the molecule and the counterelectrode can be used to switch the NDC on and off. As dispersive two-dimensional electronic states are widely available in metals and semiconductors, and moreover may be controllably modified through artificial nanostructures or molecular adlayers, our findings should simplify NDC engineering in atomic-scale metal-organic junctions.

*Present address: Institut für Experimentalphysik, Freie Universität Berlin, 14195 Berlin, Germany.
†limot@ipcms.unistra.fr.

[1] J. Chen, M. A. Reed, A. M. Rawlett, and J. M. Tour, Science **286**, 1550 (1999).
[2] J. Gaudioso, L. J. Lauhon, and W. Ho, Phys. Rev. Lett. **85**, 1918 (2000).
[3] N. J. Tao, Nature Nanotech. **1**, 173 (2006).
[4] L. Esaki, Phys. Rev. **109**, 603 (1958).
[5] I.-W. Lyo and P. Avouris, Science **245**, 1369 (1989).
[6] P. Bedrossian, D. M. Chen, K. Mortensen, and J. A. Golovchenko, Nature (London) **342**, 258 (1989).
[7] *Resonant Tunneling in Semiconductors*, edited by L. Chang, E. Mendez, and C. Tejedor (Plenum, New York, 1991).
[8] Y. Xue et al., Phys. Rev. B **59**, R7852 (1999).
[9] N. P. Guisinger et al., Nano Lett. **4**, 55 (2004).
[10] L. Chen et al., Phys. Rev. Lett. **99**, 146803 (2007).
[11] C. Zeng et al., Appl. Phys. Lett. **77**, 3595 (2000).
[12] K. J. Franke et al., Phys. Rev. Lett. **100**, 036807 (2008).
[13] M. Grobis, A. Wachowiak, R. Yamachika, and M. F. Crommie, Appl. Phys. Lett. **86**, 204102 (2005).
[14] F. D. Novaes et al., arXiv:1101.3714v1.
[15] G. Schull, T. Frederiksen, M. Brandbyge, and R. Berndt, Phys. Rev. Lett. **103**, 206803 (2009).
[16] L. Gross et al., Phys. Rev. Lett. **107**, 086101 (2011).
[17] S. D. Kevan and R. H. Gaylord, Phys. Rev. B **36**, 5809 (1987).
[18] See Supplemental Material at http://link.aps.org/supplemental/10.1103/PhysRevLett.107.246801 for spectra acquired with a C_{60}-terminated tip above surfaces or nanoscale objects other than Cu(111).
[19] X. Lu et al., Phys. Rev. Lett. **90**, 096802 (2003).

[20] C. Silien, N. A. Pradhan, W. Ho, and P. A. Thiry, Phys. Rev. B **69**, 115434 (2004).

[21] W. W. Pai *et al.*, Phys. Rev. Lett. **104**, 036103 (2010).

[22] N. Néel, L. Limot, J. Kröger, and R. Berndt, Phys. Rev. B **77**, 125431 (2008).

[23] M. V. Rastei *et al.*, Phys. Rev. Lett. **99**, 246102 (2007).

[24] G. Schull and R. Berndt (private communication).

[25] X. W. Tu, G. R. Mikaelian, and W. Ho, Phys. Rev. Lett. **100**, 126807 (2008).

[26] C. J. Chen, Phys. Rev. B **42**, 8841 (1990).

[27] Simulations also show that NDC is favored when the energy position of the surface-state onset is comparable to the width of the LUMO + 1, which is indeed the case in the present setup.

[28] I. D. Hands, J. L. Dunn, and C. A. Bates, Phys. Rev. B **81**, 205440 (2010).

[29] R. L. Carter, *Molecular Symmetry and Group Theory* (John Wiley & Sons, New York, 1998).

Supplementary material for "Engineering Negative Differential Conductance with a C_{60}-Terminated Tip"

B. W. Heinrich,[1, *] M. V. Rastei,[1] D.-J. Choi,[1] T. Frederiksen,[2] and L. Limot[1, †]

[1]*Institut de Physique et Chimie des Matériaux de Strasbourg, CNRS, Université de Strasbourg, F-67034 Strasbourg, France*
[2]*Donostia International Physics Center (DIPC), E-20018 Donostia-San Sebastián, Spain*
(Dated: July 22, 2011)

We present here additional dI/dV spectra acquired with a C_{60}-terminated tip. The tip apex was monitored through constant-current images of a Au atom, the image exhibiting a molecular pattern matching the LUMO+1 for biases close to -1.9 V. The tip apices employed were selected so to have an orientation corresponding to a C_{60} adsorbed on a corner carbon atom [Fig. S1(a)—(b)]. This orientation produces Negative Differential Conductance (NDC) in the spectra below the LUMO+1 resonance when the tip is positioned above Cu(111) [see Fig. 1 in the Letter].

In order to verify if counterelectrode selection is crucial to NDC, we also positioned the C_{60}-terminated tip above nanoscale objects other than Cu(111). These include a Au atom adsorbed on Cu(111), and, as shown on Fig. S1(c), cobalt islands grown on Cu(111) as well as C_{60} molecules adsorbed on Cu(111) or on the cobalt islands. We also replaced the Cu(111) surface with a Cu(100) surface. The corresponding dI/dV spectra are presented in Fig. S2(a). The LUMO+1 is still detected, but the spectroscopic fingerprint changes with counterelectrode nature. In Fig. S2(b) we present for the sake of comparison the same spectra acquired with a copper-coated tip. The nanoscale objects have marked electronic structure. The C_{60} molecule is governed by the HOMO, LUMO and LUMO+1 molecular resonances [1], the cobalt islands by minority d-resonances [2], the Au atom by atomic-like resonances (d_{z^2} resonance below -2 V, sp_z resonance above 2 V) [3, 4]. The Cu(100) surface, on the contrary, has a featureless electronic structure.

From Fig. S2(a) it is evident that no NDC is present below the LUMO+1. This clearly indicates that the electronic structure of Cu(111) favors NDC despite the absence of narrow energy states on this surface.
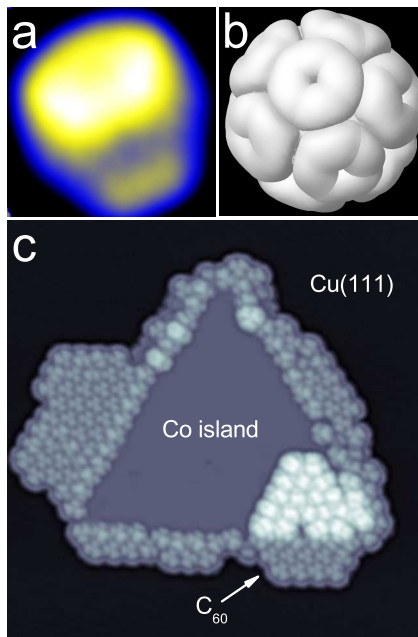

FIG. S1: (color online). (a) Constant-current image of a Au atom using a C_{60}-terminated tip (sample bias: -2.0 V, current: 0.1 nA, size: 12×12 Å^2), and, (b) Corresponding simulation of the LUMO+1 (C_{60} adsorbed on a corner carbon atom). (c) Constant-current image of C_{60} and of a cobalt island acquired with a copper-coated tip (1.9 V, 0.5 nA, 250×250 Å^2). The triangularlike islands were grown on Cu(111) at room temperature by evaporating about 0.7 monolayers (ML) of Co at 0.15 ML min^{-1}. The C_{60} molecules were dosed onto the surface after island growth. The cobalt island, the copper surface and the C_{60} molecules are labeled for clarity.
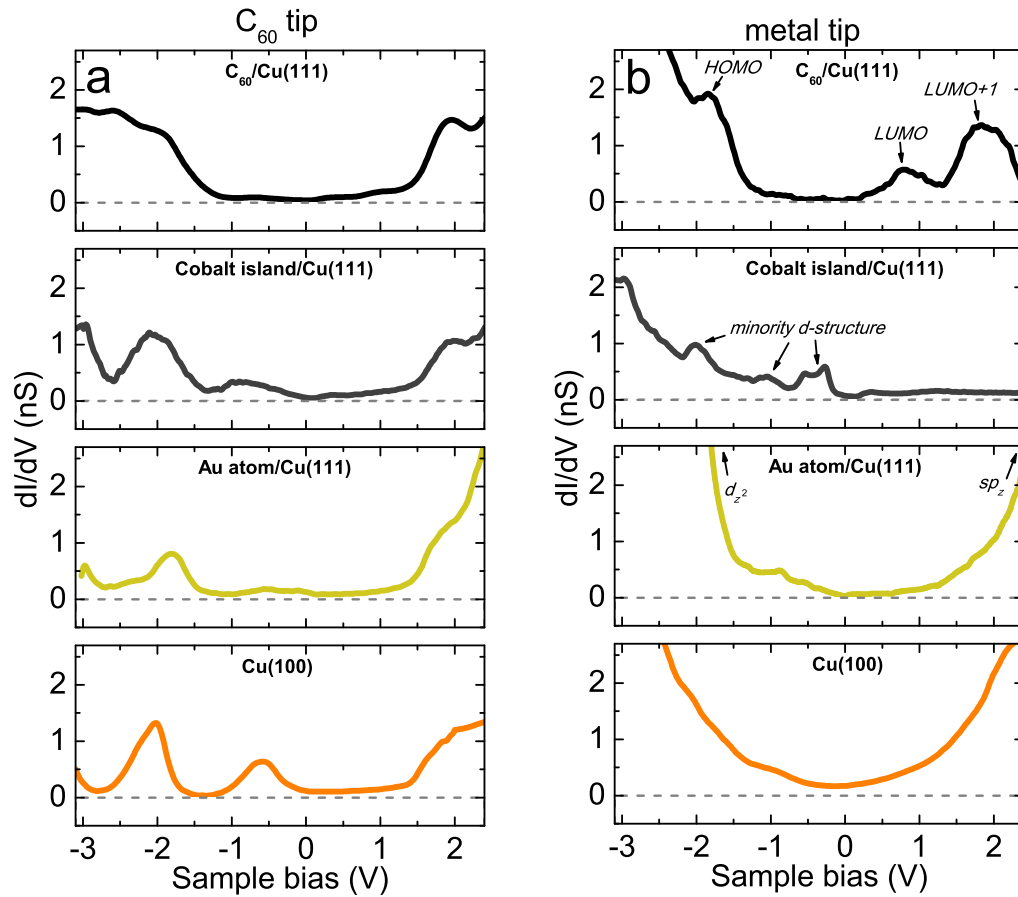
FIG. S2: (color online). (a) dI/dV spectra acquired with a C_{60}-terminated tip (corner orientation) above, from top to bottom, a C_{60} molecule on Cu(111), a cobalt island on Cu(111), a Au atom on Cu(111), and a Cu(100) surface (feedback loop opened at 1.0 V, 0.1 nA). (b) Same spectra as in (a) but acquired with a copper-coated tip. The arrows highlight the electronic structure of these nanoscale objects.

[1] X. Lu, M. Grobis, K. H. Khoo, S. G. Louie, and M. F. Crommie, Phys. Rev. Lett., **90**, 096802 (2003).

[2] M. V. Rastei *et al.*, Phys. Rev. Lett. **99**, 246102 (2007).

[3] F. E. Olsson, M. Persson, A. G. Borisov, J.-P. Gauyacq, J. Lagoute, S. Fölsch, Phys. Rev. Lett. **93**, 206803 (2004).

[4] J. Lagoute, X. Liu, and S. Fölsch, Phys. Rev. Lett. **95**, 136801 (2005).